Available online at www.sciencedirect.com

ScienceDirect

Procedia Engineering 63 (2013) 370 – 378

Procedia Engineering

www.elsevier.com/locate/procedia

The Manufacturing Engineering Society International Conference, MESIC 2013

Scanning space analysis in Selective Laser Melting for CoCrMo powder

Y. Pupo[a], J. Delgado [a], L. Serenó[a], J. Ciurana[a,*]

[a] Department of Mechanical Engineering and Industrial Construction. Universitat de Girona, Maria Aurèlia Capmany 61, 17071 Girona, Spain.

Abstract

Selective Laser Melting has been one of the last generation technologies of additive manufacturing. So far, one of the major problems confronted by researchers and designers has been the standardization of the optimal parameters. The setting of the appropriate parameters can lead to the acquisition of the desired characteristics in terms of morphology, porosity, hardness, and mechanical properties of the final piece. Therefore, the objective of this work is to study the scanning space that allows the formation of a continuous layer of material through the modification of the process parameters. Experiments were carried out in a self-develop SLM machine using CoCrMo powder as material. The experimental results showed that small separation between tracks provided a good overlapping while with higher separations, such as 750 μm, isolated tracks were produced. Furthermore, other process parameters involved in the morphology of the tracks were identified and the overlapping estimated.

Selection and peer-review under responsibility of Universidad de Zaragoza, Dpto Ing Diseño y Fabricacion

Keyword: Selective Laser Melting; metallic powder; scanning space; overlapping rate; geometrical parameters.

1. Introduction

The development of new technologies requires an improvement of the manufacturing processes in order to accelerate the product development cycle. Some additive manufacturing technologies (AM) have been developed during the last years.

* Corresponding author: Tel.: +34 972 418 829; fax: +34 972 418 098.
E-mail address: quim.ciurana@udg.edu

Selection and peer-review under responsibility of Universidad de Zaragoza, Dpto Ing Diseño y Fabricacion
doi:10.1016/j.proeng.2013.08.228

Nomenclature

φ	overlapping rate
W	track width
S	scanning space
L	layer total distance
S	scanning space
W	track width
n	number of the tracks

Selective Laser Melting (SLM), one of the most promising AM technologies, meets the manufacturing demands of time and cost reduction. It is based on the deposition of metallic powder, free of binders and fluxing agents, which is heated by a laser beam until the powder melts first and becomes a solid part after cooling down, (Vandenbroucke and Kruth, 2007). The fields of SLM applications more common are: biomedical applications, mechanical engineering, and the aerospace sector (Delgado et al. 2012). Many of the products currently manufactured by this technology are made in commercial machines that only allow the variation of very few process parameters and the use of a limited range of materials. Therefore, the development of more flexible machines can help to increase the range of applications of these technologies (Levy et al. 2003 and Dimitrov 2006).

So far, several SLM process parameters have been analyzed for single track in different works. Single track experiments provide a theoretical support for multi-track and multi-layer experiments. Over 130 factors that affect the sintered parts have been defined and 20 of them are considered as important factors (Elsen et al. 2008 and Wang et al. 2012). Most of factors are sub-processes such as heat transfer, energy absorption, and melting and solidification temperatures. However, there are 10 parameters that are repeated in all literature and that can be considered controllable. An optimal combination of them can generate better results and therefore the possibility to increase the applications for SLM. Some of them are: laser power (P), scanning speed (SS), layer thickness (LT), scanning space (S), spot size (d), particle size, oxygen content, powder temperature, etc.

The works concerning process parameters found in the literature were based on experiments mainly made on stainless steel 316L and 904L. Many authors have also worked in the description of the thermal effects, the vaporization of the metal in the melting, the type of substrate used, the conditions in work atmosphere, and capillary instability. Moreover, they deeply analyzed the morphology of single tracks to determine the effect of each input parameter (Gusarov et al. 2007). However many things remain unexplained such as the behavior of SLM using different materials, because each material has different properties and will respond differently to the same process. Currently, some research is being done, especially with new materials such as biomaterials, to increase the applications of SLM (Vandenbroucke and Kruth 2007).

The aim of this work is to evaluate the most influencing process parameters of the selective laser melting (SLM) technology, including the scanning space (S). Moreover, the limit of continuity (melted zone vs. non-melted zone) will be determined and quantified through the overlapping rate. The main goal of this study is to define the optimal process parameters in order to enhance the performance of the SLM technology. Finally, overlap with different scanning space was checked by means of overlapping calculation.

2. Experimental Procedure

2.1 Equipment

Experiments were carried out on a Kondia HS-1000 vertical milling machine equipped with an YW30 Prodintec welding head mounted and aligned in the vertical (Z) axis of the Kondia machine. The welding head had a focal length of 125 mm, and the minimum spot size produced with this configuration was 150 µm. The laser used was a FLx50s Ytterbium fiber type (Rofin-Baasel, Spain) that reached a maximum power of 500W in continuous wave and operated at a wavelength of 1080 nm Figure 1.

2.2 Material

The material used in the experimentation was a Cobalt, Chromium, Molybdenum (CoCrMo) powder with a composition of 60.24 % Co; 31.62 % Cr; 8.14 % Mo. The shape of the powder particles was predominantly spherical with diameters mostly between 20 to 50 microns. This alloy is biocompatible and has been used in previous studies with SLM process for the manufacturing of medical devices (Delgado et al. 2012).

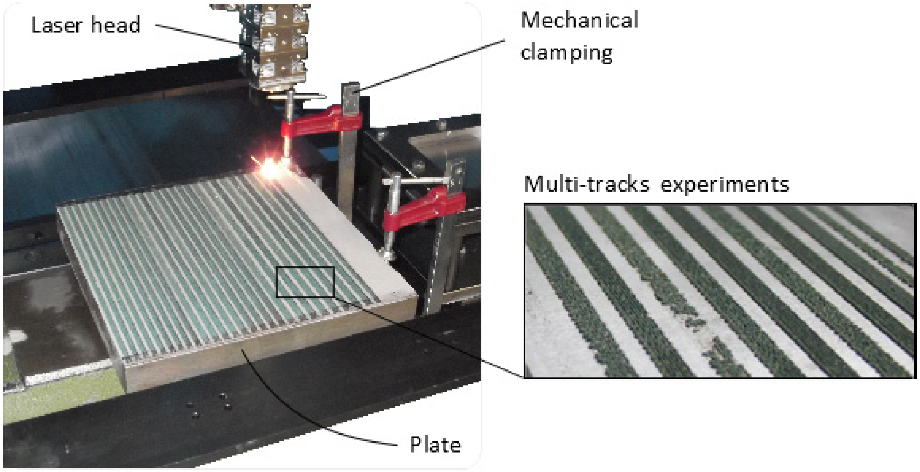

Fig. 1. Experimental equipment setting and process of Multi-tracks experiments.

2.3 Formation Process

The CoCrMo metallic powder was deposited into a sloped powder bed platform. The slope of the platform allowed obtaining continuous layer thicknesses (LT) between 40 to 500 µm. The metal powder melting process was done through a laser trajectory on both directions (forward and backward in the X-axis) in order to analyze the heat accumulation on the material during the layer formation. The experimentation was done in a non-controlled atmosphere, and therefore, the oxidation of the metallic powder was dismissed.

2.4 Design of experiments

A full factorial design was used to obtain 27 multi track of melted material. Each multi track was composed of 8 continuous single tracks formed using combinations of three different process parameters such as laser power (P), scanning speed (SS), and scanning space (S). These parameters were chosen based on previous work (Delgado et al 2012).

Based on efficiency process, heat transfer could not be too high because it causes residual stress on materials. Thus, (S) value is decided to ensure uniform distribution when several single tracks are processed. Multi-track experiments are carried out with planar and continuous optimal shape meaning overlapping (φ) from 10 up to 30 %. With that overlapping value, scanning space (S) calculation is ensured to be optimal.

Equation (1) is utilized to obtain S. (W) can be determined by mean values in each multi-track sample from experimental work where each multi-track is obtained with different process parameters. (W) Values could be from 410 y 620 microns.

A full factorial design was used to determine the effects of power, scanning speed, and scanning space. The factors and factor levels are summarized in Table 1.

Finally, 27 multi tracks made of 8 continuous single tracks and using different values for the three process parameters (P, SS, S) were obtained. Each multi track was processed. First, they were cut obtaining 10 samples for each multi track. The cuts were made based on layer thickness values – from 50 to 500 µm. The samples were then prepared using a standard metallographic process. The 270 samples were observed using an optical microscope with a measuring scale of 2000 microns. Thus geometric measures of the profiles were obtained.

Table 1. Design of experiments: parameters of the multi-track

Parameters	**value #1**	**value #2**	**value #3**
P (W)	200	300	400
SS (mm/s)	35	50	65
S (µm)	450	600	750

3. Results and discussion

The general purpose of the experiments is to study the effect of scanning space on surface morphology during SLM. Based on current experimental results, when S increases, gap between two neighboring tracks also increases leading to their isolation. Once the experiment was performed and the multi tracks formed, a thorough analysis of the micrographs acquired was carried out Figure 2. The images were evaluated from a top view and from the cutting plane. An analysis of variance (ANOVA) was carried out to assess the main effects of the process parameters (S, P, SS) on the overlapping rate. Analyzing results can be said that S affects mostly the overlapping percentage.

3.1 Analysis of layer continuity

The 270 images obtained were carefully analyzed and three categories were distinguished according to the quality of the layer:

- 1= Continuous layer of melted material (overlapping of single tracks)
- 2= Continuous single tracks of melted material, no overlapping present on the single tracks
- 3= Non-continuous single tracks (balling effect and/or no-melting)

In the continuous layer cases, the incidence of the laser over the powder single tracks provoked the melting of the material in a planar manner. In the non-continuous cases, several problems were observed: non-continuity of the track, balling effect, and/or lack of melting. These non-continuous tracks were rejected. For some continuous single tracks, it was observed a good quality of the melted material but without overlapping between the tracks. For those cases, the scanning space (S) value, meaning the distance between one single track and the subsequent, was too large to induce the overlapping between the single tracks. Those samples were further analyzed to obtain the optimal S value for each case study.

Figure 3 illustrates the results of the layer continuity analysis, where number 1 (clear grey) denotes the samples with continuous layer of melted material (with overlapping). Number 2 (dark grey) indicate the continuous single tracks of melted material but without overlapping between single tracks. Number 3 (white) stand for the samples with non-continuous tracks. In Figure 3 it can be seen that low values of scanning space (S = 450 and 600 µm) promoted the formation of continuous melted tracks (clear grey). Otherwise, when increasing S values the possibility of finding continuous tracks decreased.

Afterwards, the layer thickness was analyzed for each different S values. Figure 4a and 4b and Figure 5 plots the results obtained in Figure 3, were the continuous lines represent the samples were the melted material formed a continuous layer (with overlapping); besides the discontinuous lines mean that the sample was composed by continuous single tracks but without a overlapping between them. The absence of dots in the graph means that the obtained sample presented non-continuous single tracks, and therefore, they were rejected.

The figures suggests that a combination of a lower scanning space value (S = 450 µm), a high power (P = 400 W) and a low scanning speed (SS = 33.3 mm/s) induces the overlapping in samples with higher layer thickness (LT = 500 µm). Moreover, when increasing S values and maintaining constant the rest of parameters (P and SS), the LT obtained for each sample decreased. Therefore, the optimal values for each parameter – suitable to obtain samples of uniform material melted (with overlapping) – were: low scanning speed (SS = 33.3 mm/s), high power (P = 400 W), and low scanning space (S = 450 µm).

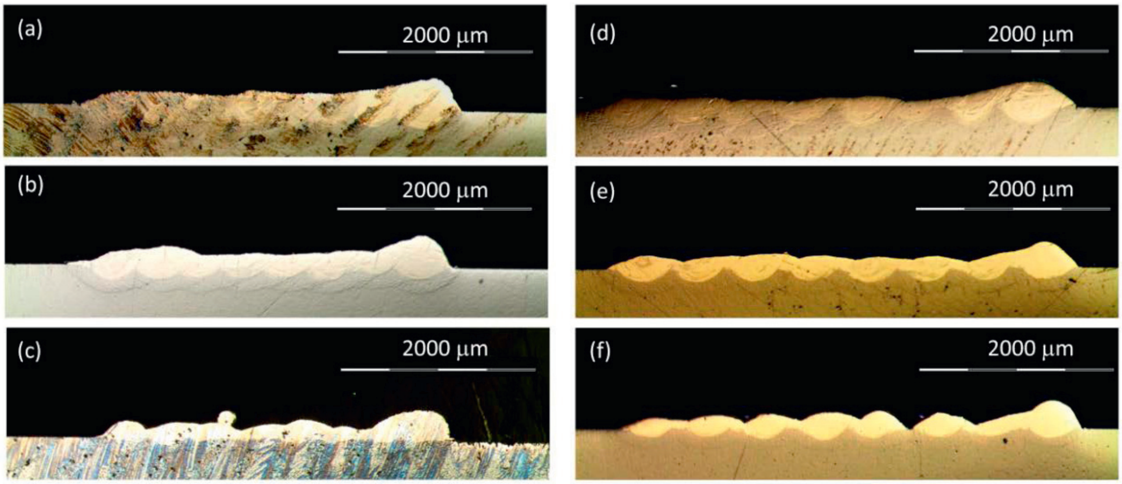

Fig. 2. Cross sections (profiles) taken perpendicular to the scanning direction of parts produced with P= 400 W, LT = 200 µm to S = 450 µm SS = 33.3 mm/s (a), S = 450 µm SS = 50 mm/s (b), S = 450 µm SS = 66.6 mm/s (c), S = 600 µm SS = 33.3 mm/s (d), S = 600 µm SS = 50 mm/s (e) and S = 600 µm SS = 66.6 mm/s (f)

SS (mm/s)	P (W)	S 450 (µm)										S 600 (µm)										S 750 (µm)									
66,6	400	1	1	1	1	3	3	3	3	3	3	1	1	1	3	3	3	3	3	3	3	2	2	3	3	3	3	3	3	3	3
	300	1	1	1	1	1	1	3	3	3	3	3	3	3	3	3	3	3	3	3	3	3	3	3	3	3	3	3	3	3	3
	200	1	1	3	3	3	3	3	3	3	3	3	3	3	3	3	3	3	3	3	3	3	3	3	3	3	3	3	3	3	3
50	400	1	1	1	1	1	1	1	1	3	3	1	1	1	1	1	1	1	3	3	3	1	1	1	1	2	2	3	3	3	3
	300	1	1	1	3	3	3	3	3	3	3	1	1	1	3	3	3	3	3	3	3	2	2	3	3	3	3	3	3	3	3
	200	3	3	3	3	3	3	3	3	3	3	3	3	3	3	3	3	3	3	3	3	3	3	3	3	3	3	3	3	3	3
33,3	400	1	1	1	1	1	1	1	1	1	1	1	1	1	1	1	1	1	1	3	3	1	1	1	1	2	2	2	2	2	2
	300	1	1	1	1	1	1	1	3	3	3	1	1	1	1	3	3	3	3	3	3	1	1	1	2	2	3	3	3	3	3
	200	1	3	3	3	3	3	3	3	3	3	3	3	3	3	3	3	3	3	3	3	2	2	3	3	3	3	3	3	3	3
LT (µm)		50	100	150	200	250	300	350	400	450	500	50	100	150	200	250	300	350	400	450	500	50	100	150	200	250	300	350	400	450	500

Fig. 3. Design of experiments. SS = scanning speed; P = laser power; S = scanning space. Number 1 (clear grey) = overlapping; Number 2 (dark grey) = non-overlapping; Number 3 (white) = non-melted

With the results obtained, the limit between samples with good overlapping and samples with no overlap was determined. Figure 4 shows a chart of the comparison of the layer thickness and laser power values for different samples. Continuous lines represent samples with smooth surfaces and overlapping between tracks. Discontinuous lines symbolize samples with good track geometry but with poor overlapping due to a non-optimal scanning space values. Again, samples with high P, low SS, and low S present a large LT. However, LT decreases while S increases.

Samples with low scanning spaces (S = 450 µm) showed the best performance, regardless of the power or the scanning speed used. The underlying principle for these results lies in the heat accumulation effect. Since the distance between tracks is low, the heat from the first track melting is still present when the laser beam is melting the following track, so it amasses. This accumulation reduces the cooling of the layer and promotes the formation of a homogeneous and continuous layer with a good overlapping.

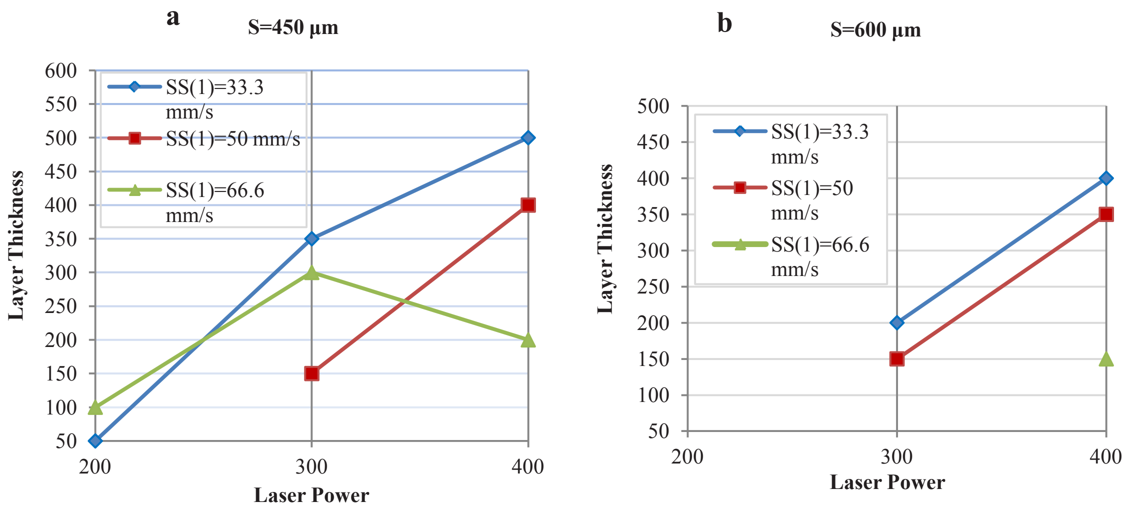

Fig. 4. Analysis of the samples obtained. (a) When P=400 W with S = 450 µm and (b) S=600 µm.

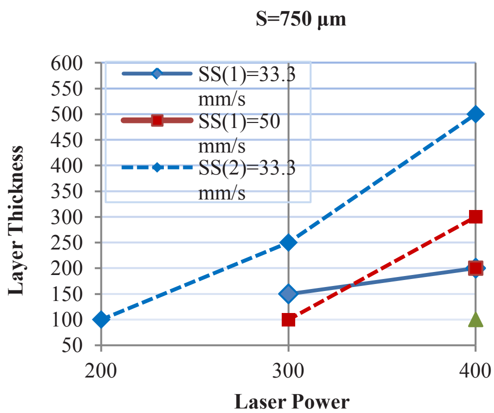

Fig. 5. Analysis of the samples obtained. S=750 µm Continuous layer = overlapping; discontinuous layer = non-overlapping.

3.2 Overlapping rate

Some authors have mentioned the term overlapping in previous works; however the way of obtaining it is few reasoned (Li et al. 2012 and Yadroitsev et al. 2007). To calculate the overlapping, it is important to take into account that it depends on the distance between laser center and single track width, expressed in percent (Equation 1) (Wang et al. 2012 and Yadroitsev et al. 2010). This work proposes a methodology to calculate this parameter based on the calculation of the width of multi-tracks.

As indicated in Figure 5, narrow tracks decreased the percentage of overlapping, causing their isolation. The consolidated solid metal absorbs less laser energy than the loose powder. The laser beam directly interacts with the powder, the substrate (effect of substrate denudation) and the previously synthesized track or only with the substrate and the previously synthesized track. A molten pool has higher levels of reflectivity than raw powder. The absorbed energy reheats the previously synthesized track or the substrate. The heat is conducted further through the substrate causing sintering/melting of the powder particles. Owing to the substrate denudation, the second track height is lower than the first one, and the zone of powder consolidation also diminishes. A top view of the samples obtained was enough to observe visually the overlapping effect. However, in order to quantify it, Equations 2 and 3 were applied. As shown, the scanning space (S) parameter was used to determine the overlapping rate.

Figure 6 shows how to calculate the parameters. For a given distance (L), three different morphologies can be obtained: a homogeneous layer of material melted (with overlapping), several tracks of material melted but without overlapping, and different tracks of melted material but separated between them. The track width (W) was determined as the distance between the center of the track and the end of the melted zone. The scanning space (S) was considered as the distance between the centers of two consecutive tracks.

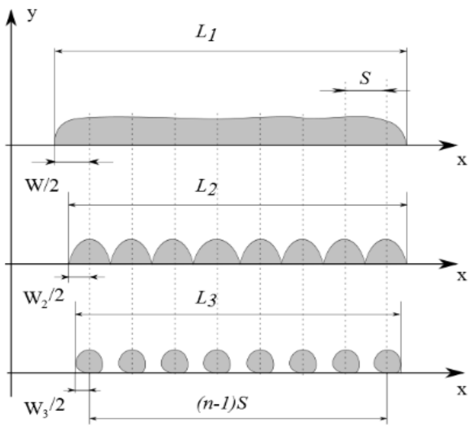

Fig. 6. Scheme of the geometrical parameters to estimate the overlapping.

When applied equations 2 and 3, overlapping values are obtained, as shown in the following figures. Thus, it can be clearly seen that the overlapping of the experimental results are similar to the simulated in design of experiments (10 and 30 %) (Wang et al. 2012). Three different scanning space values (S = 450 μm, S = 600 μm and S = 750 μm) and three laser powers (P= 200 W, P = 300 W and P = 400 W) were used to analyze the overlapping rate in each layer thicknesses for several scanning speeds (SS = 33.3 mm/s, SS = 50 mm/s, and SS = 66.6 mm/s).

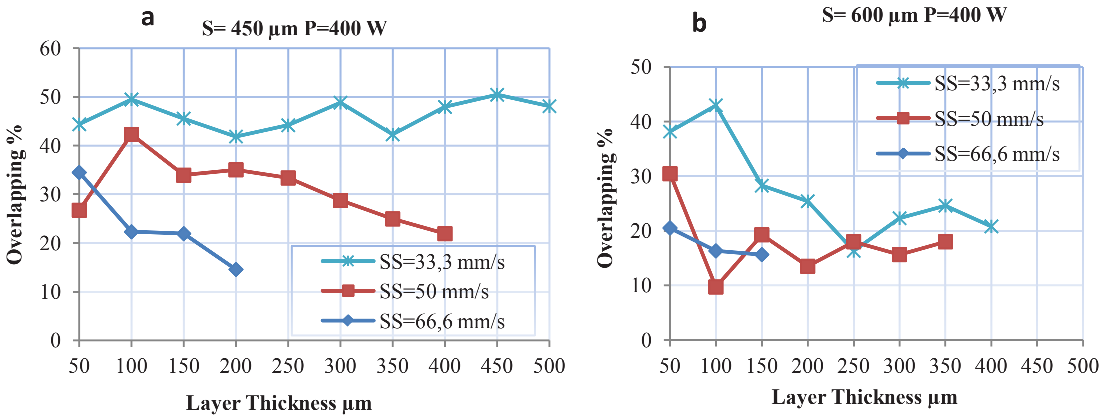

Fig. 7. Overlapping using 3 values of SS. (a) When P=400 W with S = 450 µm and (b) S=600 µm.

To P = 400 W Figure 7a and 7b, the overlapping rate goes between (10 and 50) %, with an average value of 26%. For samples with S = 450 µm, the overlapping rate is greater. Moreover, for SS = 33.3 mm/s the overlapping rate is also larger. As shown in Figure 8a and 8b, for P = 300 W the overlapping decreased notably between (-5 and 45) %.

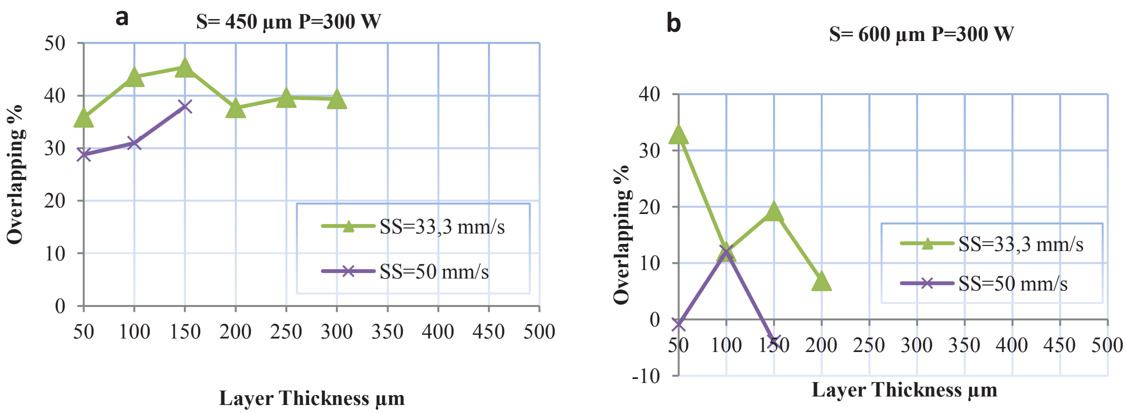

Fig. 8. Overlapping using 3 values of SS. (a) When P=300 W with S = 450 µm and (b) S=600 µm.

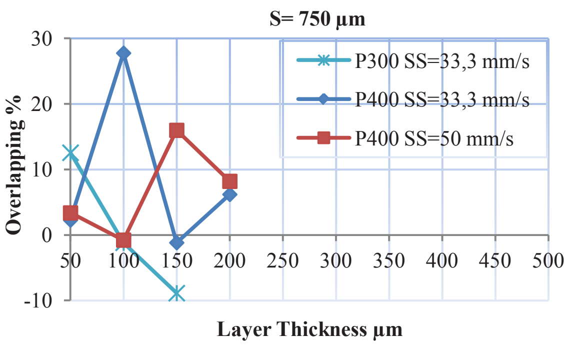

Fig. 9. Overlapping with 3 values of SS and P.

With S = 750 µm, the continuity of the powder layer thickness does not reach 200 µm. Moreover, overlapping decreased considerably (-10% and 28%), as shown in Figure 9. Therefore, the adequate selection of an optimal and minimal scanning space (S) parameter would allow obtaining continuous and homogeneous layers of melted material, improving the performance of the SLM technology. The scanning space (S) parameter was determined as one of the most important parameters to control in order to increase the efficiency of the SLM technology, demonstrating that the accumulation of energy during SLM allows an increase of overlapping when SS is low.

4. Conclusions

The relationship between three selective laser melting (SLM) process parameters and the quality of the layers produced was evaluated. Firstly, the type of surface obtained (continuous with overlapping single tracks, continuous without overlapping single tracks, and discontinuous) was determined and the limit of continuity was defined. Finally, this limit of continuity was quantified through the overlapping rate, and the most influencing process parameter, scanning space (S) was exposed.

It can be concluded that overlapping of experimental values are similar to the simulated in design of experiments except in S=750 μm and S= 600 μm with SS= 50 mm/s. The surface morphology is strongly affected by the scanning space parameter due to the heat accumulation at the melted zone. Additionally, with reduced scanning spaces the heat accumulation was greater and the overlapping rate larger.

Finally, the map of continuity obtained in this study could be used in further works in order to produce layers of different sizes and surface characteristics, increasing the range of applications of the selective laser melting technology.

References

Delgado J., Sereno L., Ciurana J. and Hernandez L., 2012. Influence of process parameters in the first melting layer of a building platform in a SLM machine, Innovative Developments in Virtual and Physical Prototyping – Bártolo et al. (eds) Taylor & Francis Group, London, ISBN 978-0-415-68418-7, pp. 499-502.

Delgado J., Sereno L., Ciurana J., and Hernández L., 2012. Methodology for analyzing the depth of sintering in the building platform, Innovative Developments in Virtual and Physical Prototyping – Bártolo et al. (eds) Taylor & Francis Group, London, ISBN 978-0-415-68418-7, pp. 495-498.

Dimitrov D., 2006. Advances in three dimensional printing – state of the art and future perspectives", Rapid Prototyping Journal 12/3, pp. 136–147.

Elsen M., Bender F., and Kruth J., 2008. Application of dimensional analysis to selective laser melting, Rapid Prototyping Journal 14/1, pp. 15–22.

Gusarov A.V., Yadroitsev I., Bertrand Ph. and Smurov I., 2007. Heat transfer modelling and stability analysis of selective laser melting, Applied Surface Science 254 (4), pp. 975–979.

Levy G.N., Schindel R., and Kruth J.P., 2003. Rapid manufacturing and rapid tooling with layer manufacturing (LM) technologies, state of the art and future perspectives, CIRP Annals – Manufacturing Technology 52(2), pp. 589-609.

Li R., Liu J., Shi Y., Wang L. and Jiang W., 2012. Balling behavior of stainless steel and nickel powder during selective laser melting process, International Journal of Advanced Manufacturing Technology 59 (9-12), pp. 1025–1035.

Vandenbroucke B. and Kruth J., 2007. Selective laser melting of biocompatible metals for rapid manufacturing of medical parts, Rapid Prototyping Journal13/4, pp.196–203.

Wang D., Yongqiang Y., Xubin S., Yonghua C., 2012. Study on energy input and its influences on single-track, multi-track, and multi-layer in SLM, Int. J. Adv. Manuf. Technol. 58, pp.1189–1199.

Yadroitsev I., Bertrand Ph., and Smurov I., 2007. Parametric analysis of the selective laser melting process, Applied Surface Science, Vol. 253, Issue: 19, pp. 8064-8069.

Yadroitsev I., Gusarov A., Yadroitsava I., Smurov I., 2010. Single track formation in selective laser melting of metal powders, Journal of Materials Processing Technology 210, pp. 1624–1631